Algerian Journal of Environmental Science and Technology
September edition. Vol.6. Nº3. (2020)
ISSN : 2437-1114
www.aljest.org

Continuous flow adsorption of orange acid II by coffee grounds in fixed bed column

K.mahdi*[1], K. benrachedi[1]

[1]Food Technology Research Laboratory (LRTA) Faculty of Technology University of M'hamed Bougara, Boumerdes, 35000 Boumerdes–Algeria

*Corresponding author: k.mahdi@univ-boumerdes.dz; Tel.: +213 00 00 00; Fax: +21300 00 00

ARTICLE INFO

Article History :

Received ***: 24/10/2018***
Accepted ***:16/07/2019***

Key Words:

Adsorption;
Fixed bed column ;
Coffee grounds ;
Orange acid II ;
Breakthrough curves.

ABSTRACT/RESUME

Abstract: *A continuous fixed-bed column study on coffee grounds was carried out at bed depths 0.5-2 cm, flow rates of 0.18-0.53 mL.min^{-1} with initial orange acid II concentrations of 20-100 mg.L^{-1} at room temperature. The breakthrough time of fixed-bed increased with the increase in bed depth, which permitted orange acid II to diffuse more into the interior of coffee grounds. But decreased with increasing initial concentration, and flow rate.*
The experimental data were in good agreement with both Thomas and Yoon-Nelson models.

I. Introduction

Dyes used across textile, pulp and paper, dye and dye intermediate, pharmaceutical, tannery and kraft bleaching industries are considered one of the important organic contaminants introduced to the natural water resources or wastewater streams [1].
This is alarming both from toxicological and esthetical perspectives and hence the treatment of the dye effluents before discharging them to water bodies is crucial [2].
Dyes according to their application divide to types of the vat, reactive, direct, acidic, disperse and cationic [3]. Acid orange 2 is located in a group of azo dyes [4]. Azo dyes are one of the artificial dyes important groups that are used for low cost, solubility, and high stability in many textile industries [5].
Dyes are generally resistant to light, water, oxidizing agents and many chemicals and therefore difficult to degrade once released into the aquatic systems. Azo dyes are the largest and most versatile class of organic dye-stuffs. These contain one or more azo bonds (–N=N–) as a chromophore group in association with aromatic structures containing functional groups such as –OH and –SO3H. The complex aromatic structures of azo dyes make them more stable and more difficult to remove from the effluents discharged into the water bodies [6].
The produced dye wastewaters in textile industries are usually toxic, non-biodegradable and resistant in the environment [7]. The discharge of dye wastewaters in the receiving waters led to the eutrophication phenomenon [8]. Dyes have the property of carcinogenic and mutagenic and cause allergy and skin problems too [8]. Direct discharge of textile industry wastewater, into the sewage or in the environment causes the sludge formation layers with containing fiber [9].
Because of the very low biodegradation ability, the existence of dye-making materials, detergents, and glues in textile wastewater disrupts the biological treatment process [6,9]. The resistance of dyes against detergent materials, sunlight, and oxidation is the cause of its low removal in the conventional treatment systems [9]. There are various methods for dye removal from wastewater. These methods consist of coagulation and flocculation, biological treatment, chemical oxidation, electrochemical treatment, ion exchange and adsorption [10,11]. The adsorption process has been noticed nowadays for low cost, facility in operation and insensibility into toxic material as a suitable technique in the removal of dye, but the usage of expensive adsorbents can be reckoned a limiting factor [11]. Different adsorbents such as activated carbon, date fibers, sawdust, grain chaff, rice husk, and cytosine have been used for dye removal [12]. The activated carbon as the most common and most efficient adsorbent material has been known, but because of the high costs production and reduction, its commercials' form in

the developing countries cannot use as a proper option.

Large quantities of coffee grounds are generated each year and constitute a significant source of agricultural waste. Such by-products corresponding to this loss are however likely to be of considerable economic interest. It proves, thus, important to develop such waste. To work out adsorbent materials starting from agricultural waste makes it possible on the one hand to eliminate them and on the other hand to optimize the output and the manufacturing costs of the exploitations. The use of the coffee ground in the water treatment polluted by the industrial wastes of textiles such as the organic compounds (dyes) perhaps an interesting way of valorization of these materials.

Application of adsorption techniques for large scale wastewater treatment usually employs continuous operations, such as fixed-bed units, as this allows for large volumes of contaminated water to be treated within a shorter period. These units may be easily scaled up from laboratory to pilot unit, and the process is easy to monitor and operate [13].

The effects of main variables, such as flow rate, dye concentration and bed depth on orange acid adsorption were presented. To predict the performance in the column, the experimental data were processed with the Thomas model, Bohart-Adams model, and Yan model.

II. Materials and methods

II.1. Preparation and characterization of coffee grounds

The coffee ground used is scented soft. This waste is washed with distilled water then dried with drying oven (MELAG) with 110 °C for 24 hours It is then filtered to retain the fraction higher than 500 microns.

Characterizations of the adsorbent were carried out to understand the physicochemical properties of the adsorbent, the coffee grounds were characterized using various techniques. (Nicolet 560 FTIR) was used to record the FTIR spectrum in the range 4000 cm^{-1} – 400 cm^{-1}. The surface morphology of the adsorbent was observed by using an electron microscope with sweeping MEB (QUANTA 650) ; The crystal structure of the adsorbent was determined by X-ray diffraction (XRD) analysis using a Philips (x'pert) 2-theta diffractometer (Panalytical, Almelo, Netherlands) at a wavelength of 1.54 µm and 2-theta range 5-120º under Cu radiation.

II.2. Fixed bed column adsorption experiments

fixed-bed column adsorption experiments were out using a laboratory-scale fixed-bed column system to predict the column breakthrough (1,5 cm inner diameter and 25 cm in height) with a bed depth of 0,32 cm (0,372 g), 1cm (0,73 g), and 2cm (1,545 g), respectively. A porous sheet was attached at the bottom of the column to support the adsorbent bed. The experiments were conducted by pumping OA II solution in downflow mode through the fixed-bed column with a peristaltic pump (see **figure 1**). The temperatures of all experiments were 20°C. Samples were collected at regular time intervals in the adsorptive process. The concentration of OA II in the solution was analyzed using a UV spectrophotometer (Shimadzu UV spectrophotometer UV-1800) by monitoring the absorbance changes at a wavelength of maximum absorbance 490,5 nm.

The effects of three factors on OA II adsorption were studied: (i) solution flow rate was adjusted at 3, 5 and 8 mL min^{-1} while OA II concentration and depth were held constant at 20 $mg.L^{-1}$ and 1cm, respectively; (ii) OA II concentration was adjusted at 20, 50, and 100 $mg.L^{-1}$ with 5 mL min^{-1} flow rate and bed depth 1cm; and (iii) bed depth was adjusted at 0,5 , 1, and 2 cm with 5 mL min^{-1} flow rate and OA II concentration 20 $mg.L^{-1}$.

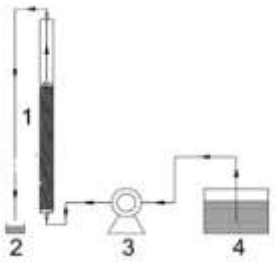

Figure 1. *Schematic diagram of a fixed-bed column*
(1) Fixed-bed column, (2) sample collector, (3) peristaltic pump and (4) sample solution

The saturation capacity for the coffee grounds in the column studies was calculated by the following equation:

$$qe = {}_0\int^{vt} (C_0\text{-}C)\, dv/m \qquad \textbf{(1)}$$

Where qe is the equilibrium OA II uptake or maximum adsorption capacity of the column ($mg.g^{-1}$), C_0 is the initial OA II concentration of the solution ($mg.L^{-1}$), C is the OA II concentration of the solution ($mg.L^{-1}$), the solution concentration (C) from the column that reaches about 10% of the initial concentration (C_0) is the breakthrough point. And t_b (min) is the time to the breakthrough point. The volume V_E(L) of solution required to reach the exhaustion point (C/C_0= 90%) in the column studies was calculated by the following equation:

$$V_E(L) = Qte \qquad \textbf{(2)}$$

Where te (min) is the time to the exhaustion point.

Algerian Journal of Environmental Science and Technology
September edition. Vol.6. N°3. (2020)
ISSN : 2437-1114
www.aljest.org

The total mass of OA II adsorbed, qtotal (mg) can be calculated by the following equation:

$$q_{total} = q_e m \quad \textbf{(3)}$$

The removal percentage of OA II can be obtained from the following equation:

$$Y(\%)=q_{total}/(C_0 V_E)x100\% \quad \textbf{(4)}$$

The (EBCT) represents the empty bed contact time

$$ECBT\ (min)= bed\ volume\ (ml)/Q(mL\ min^{-1}) \quad \textbf{(5)}$$

III. Results and discussion

III.1. characterization of adsorbent

The FTIR spectrum shown in **figure (2)** confirms the presence of these functions. For the amide function, a band around 3338 cm^{-1} is observed. There is a band around 1742 cm^{-1} for C =O stretching, for the amine function, there is a band around 1240 cm^{-1} characteristic of C-N stretching. We can also note the bands at 2922 cm^{-1} and 1644 corresponds to C = C stretching.

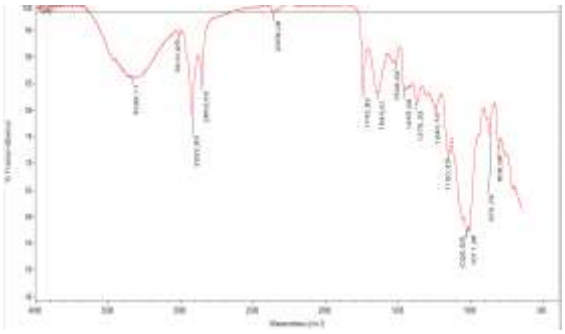

Figure 2. *Spectrum IR of coffee grounds*

Table 1. *Characterization of coffee grounds by infrared spectroscopy (IR)*

Sample	Wavenumber (cm^{-1})	Bond
Coffee grounds	3338.11	O-H bound
	2922.89	C-H
	2853.53	C-H
	1644.61	C=C aromatic
	1520.02	C=O/N-H
	1455.9	C=C
	1376.33	OH deformation
	1240.74	C-O/C-N
	1028.5	C-OH
	806.9	=C-H

Figure 3 shows the scanning electron microscopy (brand QUANTA 650) of the adsorbent (coffee grounds). As can be seen in **fig 3**, the coffee grounds surface presents a porous structure with many cavities with different size and morphology, indicating a porous structure of coffee grounds.

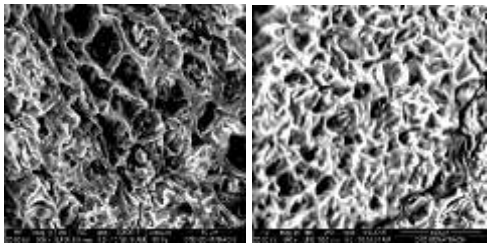

P1X500 (50 µm) ***P2X500 (100 µm)***

Figure. 3. *Photographs with the M.E.B of the coffee ground*

X-ray diffraction analyzes as a powerful tool was used to study the crystal structures of the coffee grounds, the result is shown in **figure 4**.
the six broad peaks observed in the diffractogram at around 25,71°, (37,67°, 40,41° , 43,82°), 72,19°, 88,25° correspond respectively to silicium oxide SiO_2 (hexagonal structure), calcium fluoride CaF_2 (cubic structure), calcium carbonate $CaCO_3$ (rhombohedral structure).

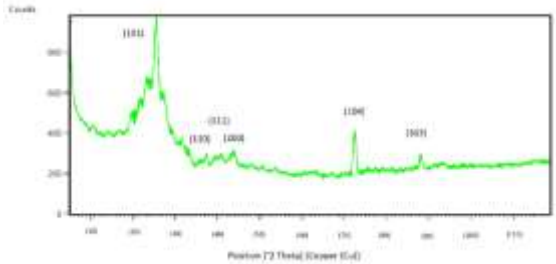

Figure 4. *X-ray diffraction (XRD) pattern of coffee grounds*

III.2. Fixed bed column adsorption experiments

III.2.1. Effect of bed depths

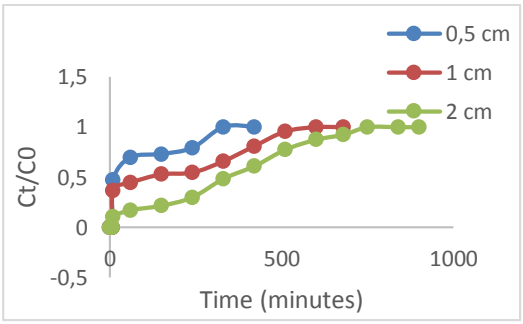

Figure. 5. *Effect of bed-depths on the breakthrough curve of OA II adsorption on coffee grounds. Conditions : Initial OA II concentration, 20 mgL^{-1}; Flow rate, 0.35 $mLmin^{-1}$; Temperature, 298K.*

The breakthrough curves at different bed depths from 0,5 to 2cm with a flow rate of 0,35 mL min^{-1} and an initial orange acid II concentration of 20 mg L^{-1} at 298 k are shown in Fig. 5. As the bed depth increased from 0.5 to 2cm, the exhaustion time (t_e) reaching exhaustion point increased from 330 to 750 min. showing that the coffee grounds bed of greater depth was saturated more slowly than that of a lower depth. Whereas the slope of the breakthrough curve decreased with the bed depths, which resulted in a broadened mass transfer zone. As shown in Table 1. with an increase in bed depth, the V_E increased due to the more contact time, and the removal efficiency (Y) of orange acid II increased from 18.6% to 99% as well. The total masses of adsorbed orange acid II (q_{total}) on coffee grounds bed were 23.09, 41.99, and 52.49mg respectively, when the bed depths were 0.5, 1, 2cm, respectively. It demonstrated that the bed depth strongly affected the total adsorbed amount of orange acid II. The increase in orange acid II adsorption with the increasing bed depth in the fixed-bed column might be due to the increased adsorbent doses in larger beds, which provided greater service area (or adsorption sites).The values of breakthrough time (t_b) obtained were 330, 300 and 240 min, respectively. The increase of breakthrough time with increasing bed depth from 0.5 to 2cm was due to the increase of EBCT from 3.39 to 10.85 min, which permitted orange acid II to diffuse more into the interior of the coffee grounds. It could be suggested that, with increasing bed depth or EBCT, the mass-transfer zone formed would move down the bed, spending more time contacting adsorbent in the column. The results obtained were found to be similar to those reported by other workers [14-17].

III.2.2. Effect of flow rates

the breakthrough curves of OA II at various flow rates from 0.18 to 0.53 Ml min^{-1} with a bed depth of 1cm and an initial OA II concentration of 10 mg.L^{-1} at 298 k are shown in **Fig. 4.** When the flow rates increased from 0.18 to 0.53 mL min^{-1}, the breakthrough time decreased rapidly from 360 to 150 min, showing that the breakthrough occurred faster with increasing flow rate. As the flow rates increased, the EBCT and the exhaustion time decreased from 10 to 3.39 min and from 750 to 360 min, respectively. It demonstrated that the flow rate affected the EBCT and the exhaustion time of the breakthrough curves. This was due to a decrease in the residence time, which restricted the contact of OA II solution to the coffee grounds [18]. At a higher flow rate, the OA II did not have enough time to diffuse into the pores of the coffee grounds and they passed the column fast before equilibrium occurred. Hence, an early breakthrough occurred, resulting in low bed adsorption capacity and low removal efficiency **(Table 2)** [19,20]. When the linear flow rate decreased, the contact time between OA II and coffee grounds in the column was longer, which favored a better adsorption capacity of coffee grounds and relative high removal efficiency **(Table 2)**.

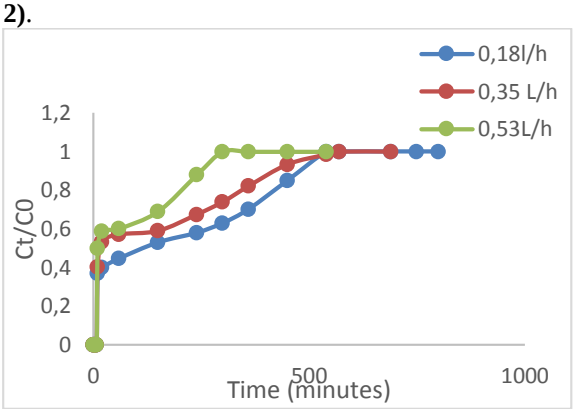

Figure 6. *Effect of flow rates on the breakthrough curve of OA II adsorption on coffee grounds. Conditions: bed depth, 1cm; initial OA II concentration, 20 mgL^{-1}; temperature, 298K.*

III.2.3. Effect of initial OA II concentrations

The effect of OA II concentrations from 20 to 100 mg.L^{-1} with a bed depth of 1cm and a flow rate of 0.35 mL min^{-1} at 298k on the breakthrough curves is shown in **Fig. 5.**

When the OA II concentrations increased from 20 to 100 mg.L^{-1}, the breakthrough time and the exhaustion time decreased from 300 to 150 min and from 600 to 300min, respectively. The adsorption process reached saturation faster and the breakthrough time appeared earlier with increasing dye concentration.

It can be explained that a higher concentration gradient caused faster transport due to an increase in the diffusion coefficient or mass transfer coefficient [21,22]. As shown in Table1. With an increase in OA II concentrations from 20 to 100 mg.L^{-1}, the maximum adsorption capacity of coffee grounds were found to increase from 41.99 to 52.49 mg.g^{-1}, which may be attributed to higher OA II concentration providing higher driving force for the transfer process to overcome the mass transfer resistance, whereas the removal efficiency decreased from 99% to 49%, which might be caused by the fast saturation of coffee grounds.

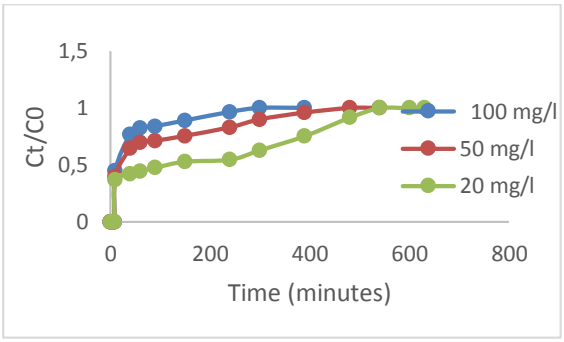

Figure. 7*. Effect of initial OA II concentrations on the breakthrough curve of OA II adsorption on coffee*

grounds. Conditions: bed depth, 1cm; flow rate 0.35 mLmin^{-1} ; temperature, 298k.

It can be explained that a higher concentration gradient caused faster transport due to an increase in the diffusion coefficient or mass transfer coefficient [21,22]. As shown in Table 2. With an increase in OA II concentrations from 20 to 100 mg.L^{-1}, the maximum adsorption capacity of coffee grounds were found to increase from 41.99 to 52.49 mg.g^{-1}, which may be attributed to higher OA II concentration providing higher driving force for the transfer process to overcome the mass transfer resistance, whereas the removal efficiency decreased from 99% to 49%, which might be caused by the fast saturation of coffee grounds.

III.3. Breakthrough curve modeling

The operation and dynamic response of an adsorption column can be predicted by the breakthrough point and shape of the breakthrough curve. In this study Bohart-Adams, Thomas and Yoon-Nelson models have been applied to determine the characteristic parameters of the column.

III.3.1. Bohart-Adams model

Bohart and Adams model described the relationship between "$\frac{ct}{c0}$ " and "t" in a continuously flowing system. The model is used for the description of the initial part of the breakthrough curve [23,24**]**. The mathematical equation of this model can be expressed as:

$$\ln\left(\frac{ct}{c0}\right) = K_{AB}\, C_0 t - K_{AB} N_0 \left(\frac{Z}{\mu 0}\right) \qquad (6)$$

Where C_0 and C_t are the inlet and outlet adsorbate concentrations (mg.L^{-1}), respectively, K_{AB} is the kinetic constant (L mg^{-1} min^{-1}), Z is the bed height (cm), μ_0 is the linear velocity (cm min^{-1}) and N_0 is the saturation concentration (mg L^{-1}). $\ln\left(\frac{ct}{c0}\right)$ Was plotted against 't' at different flow rates, bed heights and initial concentrations of orange acid II **(Figs. 8-10)**.

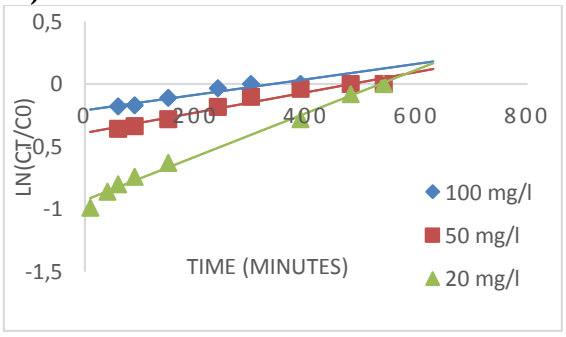

Figure 8. *Bohart-Adams plots for the adsorption of OA II onto coffee grounds: effect of initial concentration (bed height 1cm; flow rate 0.35 mLmin^{-1})*

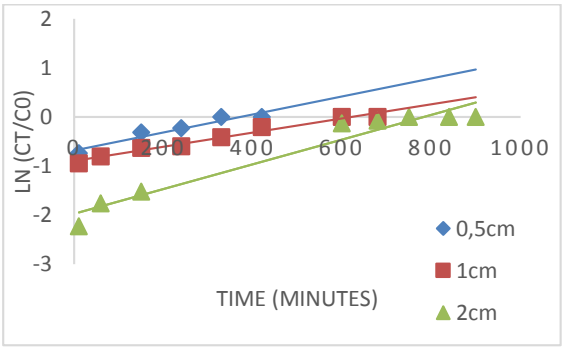

Figure 9. *Bohart-Adams plots for the adsorption of OA II onto coffee grounds: effect of bed height (initial Concentration 20mg.L^{-1}; flow rate 0.35 ml.min^{-1})*

The values of K_{AB} and N_0 were calculated from the slope and intercept of the plot, respectively. The calculated values of K_{AB} and N_0 along with the correlation coefficients (R^2) are summarized in **Table 3**. It is evident from Table 3 that the mass transfer coefficient increased with an increase in flow rate and the correlation coefficient decreased from 0.981 to 0.933. The correlation coefficients were found to be high for the study of flow rate which indicated that Bohart-Adams model is applicable for predicting the initial process of the present system. The mass transfer coefficients increased with both an increase in bed height and an initial concentration of orange acid II. The results suggested that the overall system kinetics was dominated by external mass transfer in the initial part of adsorption in the column [25].

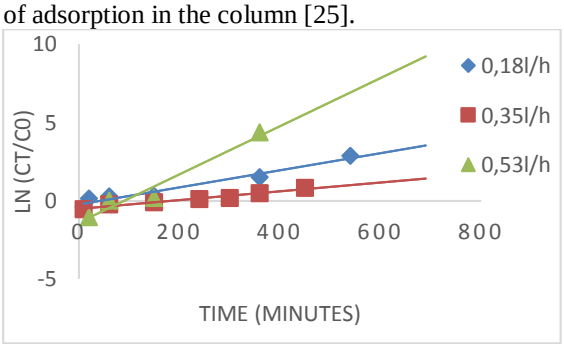

Figure. 10. *Bohart-Adams plots for the adsorption of OA II onto coffee grounds: effect of flow rate (bed-height 1cm ; initial concentration 20mg.L^{-1})*

III.3.2. Thomas model

Thomas model is one the most general and widely used model to describe the performance of the sorption process in a fixed bed column. Thomas model is expressed by the equation [26]:

$$\ln\left(\frac{C0}{Ct} - 1\right) = \frac{Kth\ q0\ m}{Q} - Kth\ C0\ t \qquad (7)$$

Where K_{th} is the Thomas rate constant (mL min^{-1} mg^{-1}), q_0 is the maximum sorption capacity (mg g^{-1}), m is the mass of adsorbent (g) and Q is the flow rate (mL min^{-1}). The values of K_{th} and q_0 can be evaluated

from the slope and intercept of the plot of $\ln\left(\frac{C0}{Ct}-1\right)$ versus 't' **(figs 11-13)**.

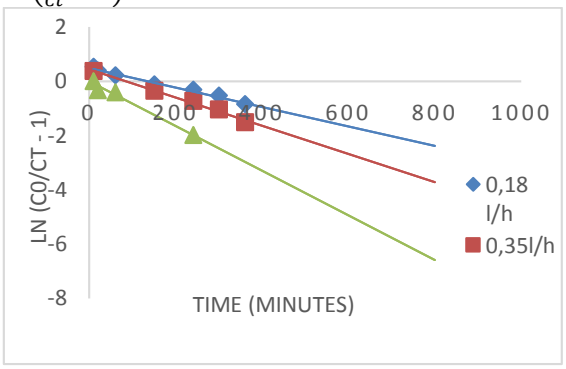

Figure 11. *Thomas plots for the adsorption of OA II Onto coffee grounds: effect of flow rate (bed height 1cm; initial concentration 20mgL^{-1})*

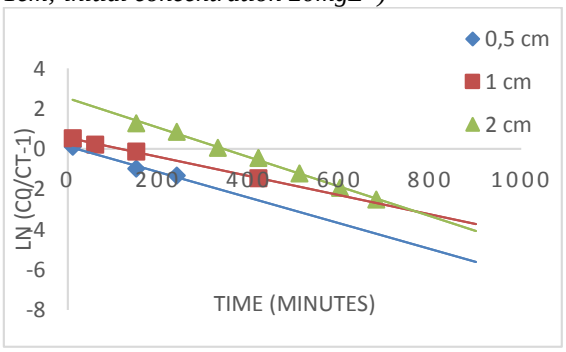

Figure 12. Thomas plots for the adsorption of OA II onto coffee grounds: effect of bed height (flow rate 0.35mLmin^{-1};initial concentration 20mgL^{-1})

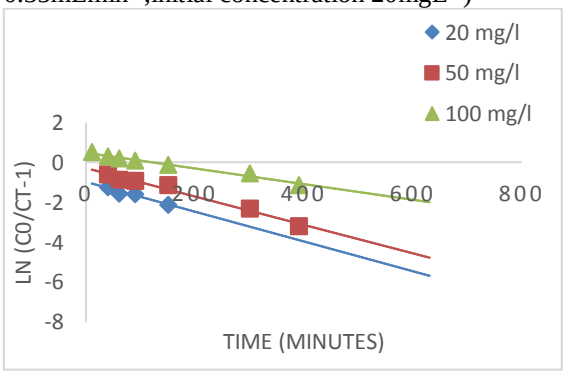

Figure. 13. *Thomas plots for the adsorption of OA II onto coffee grounds: effect of initial concentration (Flow rate 0.35 mLmin^{-1} ; bed height 1cm)*

The values of K_{th}, q_0, and R^2 are presented in table 2. As can be seen in Table 2 that the values of the correlation coefficient (R^2) vary from 0.9452 to 0.9975. The values of Thomas rate constant, K_{Th}, increased and the values of q_0 decreased with an increasing flow rate. It was also observed that the maximum sorption capacity (q_0) decreased and K_{Th} value increased with an increase in bed height. A similar trend has also been observed for the removal of Cr(VI) [27]. The experimental data fitted well to the Thomas model which indicated that the external and internal diffusion will not be the limiting step. When the initial concentration of orange acid II increased, the value of q_0 increased but the value of K_{Th} decreased. The reason is that the driving force for adsorption is the concentration difference between the adsorbate on the adsorbent and adsorbate in the solution [28].

III.3.3. Yoon-Nelson model

Yoon-Nelson model is based on the assumption that the rate of decrease in the probability of adsorption for each adsorbate molecule is proportional to the probability of adsorbate adsorption and the probability of the adsorbate breakthrough on the adsorbent. The linear form of Yoon-Nelson model is expressed as [29]:

$$\ln\left(\frac{Ct}{C0-Ct}\right) = K_{YN}t - \tau K_{YN} \qquad \textbf{(8)}$$

Where K_{YN} is the Yoon-Nelson constant (min^{-1}). τ is the time required for retaining 50% of the initial adsorbate (min) and t is the sampling time (min). Yoon-Nelson model was applied to investigate the breakthrough behavior of orange acid II adsorption onto the coffee grounds column. The linear plot of $\ln\left(\frac{Ct}{C0-Ct}\right)$ versus sampling time 't' at different flow rates, bed heights, and initial dye concentrations are shown in **Figs. 14-16**.

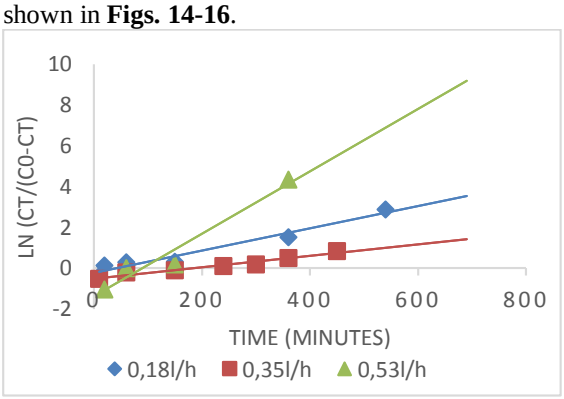

Figure 14. *Yoon-Nelson plots for the adsorption Of OA II onto coffee grounds: effect of flow rate (bed heigh 1cm; initial concentration 20 mg.L^{-1})*

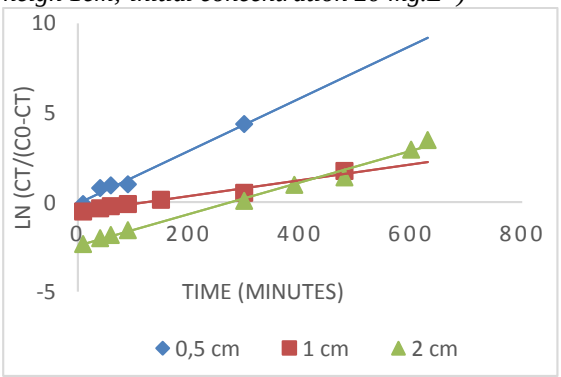

Figure 15. *Yoon-Nelson plots for the adsorption of OA II onto coffee grounds: effect of bed height (flow rate 0.35 mLmin^{-1}; initial concentration 20 mg.L^{-1})*

The values of K_{YN} and τ were estimated from the slope and intercept, respectively and summarized in Table 3. As can be seen from Table 2 that the values K_{YN} were found to increase with an increase in both flow rate and initial dye concentration whereas the

corresponding values of τ decreased. With an increase in the bed height, the K_{YN} values decreased while the τ values exhibited a reverse trend. Higher values of correlation coefficients indicated that both Thomas and Yoon-Nelson models fitted well to the experimental data.

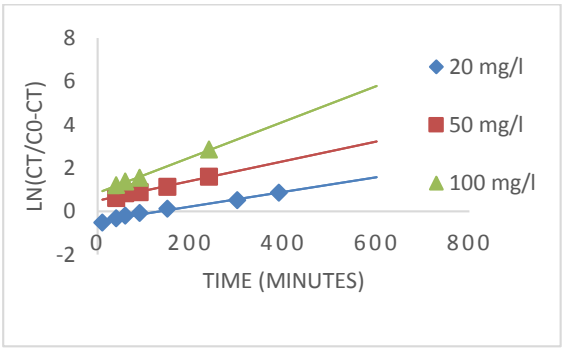

Figure. 16. *Yoon-Nelson plots for the adsorption of OA II onto coffee grounds: effect of initial concentration (flow rate 0.35 mLmin^{-1}; bed height 1cm*

Table 2. *Parameters in a fixed-bed column for OA II adsorption by coffee grounds.*

C_0 (mg L^1)	Z (cm)	Q (ml min^{-1})	EBCT (min)	T (K)	T_b (min)	T_e (min)	q_{total} (mg)	$q_{equattion}$ (mg g^{-1})	V_E (L)	Y (%)
20	*1*	0.35	5.14	308	300	600	41.99	57.29	210	99
50	1	0.35	5.14	298	240	480	156.33	114.59	168	18.6
100	1	0.35	5.14	298	150	300	52.49	71.62	105	49
20	0.5	0.35	4	298	240	330	23.09	40.38	115.5	99
20	1	0.35	5.14	318	330	600	41.99	57.29	210	99
20	2	0.35	10.85	298	330	750	52.49	34.09	262.5	99
20	*1*	0.18	10	298	360	750	50.31	36.83	135	18.6
20	1	0.35	5.14	298	360	570	39.89	54.43	199.5	99
20	1	0.53	3.39	298	150	360	37.99	51.84	190.8	99

Table. 3. Parameters of the Bohart-Adams, Thomas and Yoon-Nelson models at different conditions.

parameters		**K_{AB}(Lmg^{-1}min^{-1})**	**N_0(mg.L^{-1})**	**R^2**
Bohart-Adams model				
Flow rate (mLmin^{-1})	0.18	8.5 x 10^{-4}	43.03	0.9819
	0.35	6 x 10^{-5}	819.26	0.9828
	0.53	105 x 10^{-4}	6.88	0.9388
Bed height (cm)	0.5	9 x 10^{-5}	2237	0.9216
	1	7 x 10^{-5}	950.72	0.9733
	2	125 x 10^{-4}	2.92	0.9454
Initial concentration (mgL^{-1})	20	3 x 10^{-5}	515.91	0.9224
	50	16 x 10^{-5}	181	0.9578
	100	17 x 10^{-5}	405.32	0.9895
Thomas model		**K_{Th}(mLmin^{-1}mg^{-1})**	**q_0 (mg g^{-1})**	**R^2**
Flow rate (mLmin^{-1})	0.18	18 x 10^{-4}	8.33	0.9847
	0.35	26 x 10^{-4}	6.57	0.9901
	0.53	41 x 10^{-4}	0.075	0.9816

Bed height (cm)	0.5	32×10^{-4}	11.06	0.9917
	1	24×10^{-4}	2.057	0.9975
	2	35×10^{-4}	1.61	0.9961
Initial concentration (mgL^{-1})	20	375×10^{-4}	1.26	0.9852
	50	142×10^{-4}	0.96	0.9795
	100	39×10^{-5}	59.25	0.9781
Yoon-Nelson model		**$K_{Yn}(min^{-1})$**	**τ**	**R^2**
Flow rate ($mLmin^{-1}$)	0.18	1.53×10^{-3}	90.1	0.9559
	0.35	28×10^{-3}	18.21	0.9595
	0.53	55×10^{-3}	4.36	0.9522
Bed height (cm)	0.5	88×10^{-3}	12.25	0.9834
	1	44×10^{-3}	27.31	0.9694
	2	1.47×10^{-3}	46.61	0.9911
Initial concentration (mgL^{-1})	20	34×10^{-3}	13.23	0.9827
	50	46×10^{-3}	10.21	0.9773
	100	82×10^{-3}	10.36	0.9981

IV. Conclusion

fixed-bed column studies using coffee grounds to remove orange acid II were conducted; this study suggested that the adsorption of orange acid II was dependent on the flow rate, bed height, and initial dye concentration. The increase of breakthrough time with increasing bed depth from 0.5 to 2cm was due to the increase of EBCT from 3.39 to 10.85 min, which permitted orange acid II to diffuse more into the interior of the coffee grounds. With the increase in OA II concentrations from 20 to 100 $mg.L^{-1}$, the maximum adsorption capacity of coffee grounds was found to increase from 41.99 to 52.49 $mg.g^{-1}$.

When the flow rates increased from 0.18 to 0.53 mL min^{-1}, the breakthrough time decreased rapidly from 360 to 150 min, showing that the breakthrough occurred faster with increasing flow rate.

Thomas and Yoon-Nelson models provided a better description of experimental kinetic data in comparison to Bohart-Adams model.

In terms of perspectives, we plan to do the following work:

- Show that the natural abundance of this food waste could offer new natural support for adsorption and help to clean up wastewater.
- Make a comparative study of the adsorption capacity of coffee grounds in their native state with other adsorbents to demonstrate their industrial and economic interest.

V. References

1. Carmen, Z.; Daniel, S. Textile organic dyes-characteristics, polluting effects and separation/elimination procedures from industrial effluents-A critical overview. *Organic polluants ten years after the Stockholm convention-environnemental and analytical update* (2009) 55-86.
2. Metivier-pignon, H., Faur-Brasquet, C.; &Le Cloirec. Adsorption of dyes onto activated carbon cloths: Approach of adsorption mechanisms and coupling of ACC with ultrafiltration to treat coloured wastewaters. *Separation and purification Technology* 31 (2003) 3-11.
3. Xu, XR.; Li, HB.; Wang, WH.; Gu, JD. Degradation of dyes in aqueous solutions by the Fenton process. *Chemosphere* 57 (2004) 595-600.
4. Abramian, L.; El-Rassy, H. Adsorption kinetics and thermodynamics of azo-dye Orange II onto highly porous titania aerogel. *Chemical Engineering Journal* 10 (2009) 150-403.
5. Shirmardi, M.; Khodarahmi, F.; Heidari Farsani, M.; Naeimabadi, A.; Vosughi Niri, M.; Jafari, J. Application of oxidized multiwall carbon nanotubes as a novel adsorbent for removal of Acid Red 18 dye from aqueous solution. *Journal North Khorasan* 4 (2012) 335-47.
6. Crini, G. Non-conventional low-cost adsorbents for dye removal. *A review. Bioresouce. Technology* 97 (2006) 1061–1085.
7. Ghanizadeh, Gh.; Asgari, Gh. Removal of methylene blue dye from synthetic wastewater with bone char. *Iranian Journal of Health and Environment* 2 (2009) 104-13.
8. Asgari, Gh.; Hoseinzadeh, E.; Taghavi, M.; Jafari, J.; Sidmohammadi, A. Removal of reactive black 5 from aqueouse solutionUsing catalytic ozonation process with bone char. *Jundi Shapur Journal Health Science* 4 (2012) 21-30.
9. Saghi, MH.; Allahabadi, A.; Rahmani Sani, A.; Vaziri, T.; Hekmatshoar, R. Removal of reactive orange 3 dye from aqueous solution by biosorption technology. *Journal Sabzevar University Mohamed Science* 19 (2012) 127-35.
10. Ghaneian, MT.; Ehrampoush, MH.; Ghanizadeh, Gh.; Dehvary, M.; Abootoraby, M.; Jasemizad, T. Application of solar irradiation / K2S2O8 photochemical oxidation process for the removal of reactive blue 19 dye from aqueous solutions. *Iranian Journal of Health and Environment* 3 (2010) 165-76.
11. Bazrafshan, E.; Kord Mostafapour, F. Evaluation of color removal of Methylene blue from aqueous solutions using plant stemash of Persica. *Journal North Khorasan University Mohamed Science* 4 (2012) 523-32.
12. Ghaneian, M.; Ehrampoush, M.; Ghanizadeh, G.; Momtaz, M. Study of eggshell performance as a natural sorbent for the removal of reactive red 198 dye from aqueous solution. *Journal Toloo Behdasht* 10 (2011) 70-81.
13. Auta, M.; Hameed, B.H. Acid modified local clay beads as effective low-cost adsorbent for dynamic adsorption of methylene blue. *Journal of Industrial and Engineering Chemistry* 19 (2013) 1153- 1161.
14. Suksabye, P.; Thiravetyan, W. Column study of chromium (IV) adsorption from electroplating industry by coconut coir pith. *Journal Hazard Materiel* 160(2008) 56-62.

15. Sarin, V.; Singh, T.S.; pant, k.k. Thermodynamic and breakthrough column studies for the selective sorption of chromium from industrial effluent on activated eucalyptus bark. *Bioresource Technology* 97 (2006) 1986-1993.
16. Kundu, S.; Gupta, A.K. As (III) removal from aqueous medium in fixed bed using iron oxide-coated cement (IOCC); experimental and modeling studies. *Chemical Engeneering Journal* 129 (2007) 123-131.
17. Vijayaraghavan, K.; Prabu, D. Potential of sargassum wighti biomass for copper (II) removal from aqueous solution: application of different mathematical models to batch and cntinuous biosorption data. *Journal Hazard Materiel* 137 (2006) 558-564.
18. Sushanta, D.; Krishna, B.; Uday, C.G. Removal of Ni (II) and Cr (VI) with Titanium (IV) oxide nanoparticle agglomerates in fixed-bed columns. *Indian Engeneering Chemical Research* 49 (2010) 2031-2039.
19. Sotelo, J.I.; Ovejero, G.; Rodriguez, A.; Alvarez, S.; Garcia, J. Removal of atenolol and isoproturon in aqueous solutions by adsorption in a fixed-bed column. *Indian Engeneering Chemical Research* 51 (2012) 5045-5055.
20. Sabio, E.; Zamora, F.; Ganan, J.; Gonzalez-Garcia, C.M.; Gonzalez, J.F. Adsorption of p-nitrophenol on activated carbon fixed-bed. *Water Research* 40 (2006) 3053-3060.
21. Salman, J.M.; Njoku, V.O.; Hameed, B.H. Batch and fixed-bed adsorption of 2,4-dichlorophenoxyacetic acid onto oil palm frond activated carbon. *Chemical Engeneering Journal* 174 (2011) 33-40.
22. Kavianinia, I.; Plieger, P.G.; Kandile, N.G.; Harding, D.R.K. Fixed-bed column studies on a modified chitosan hydrogel for detoxification of aqueous solutions from copper (II), Carbohyd. *Polymer* 90 (2012) 875-886.
23. Singh, D.K.; Mohan, S.; Kumar, V.; Hasan, S.H. Kinetic, isotherm and thermodynamic studies of adsorption behaviour of CNT/CuO nanocomposite for the removal of As (III) and As (V) from water. *Research Advanced* 6 (2016) 1218-1230.
24. Reichenberg, D. Properties of ion–exchange resins in relation to their structure III Kinetics of exchange. *American Journal of Chemistry* 75 (1953) 589-592.
25. Yilmaz, M.S.; Ozdemir, O.D.; Kasap, S.; Piskin, S. The kinetics and thermodynamics of nickel adsorption from galvanic sludge leachate on nanometer titania powders. *Research Chemical Intermediate* 41 (2015) 1499-1515.
26. Ahmad, A.A.; Hameed, B.H. Fixed-bed adsorption of reactive azo dye onto granular activated carbon prepared from waste. *Journal Hazard Material* 175 (2010) 298-303.
27. Aksu, Z.; Gonen, F. Biosorption of phenol by immobilized activated sludge in a continuous packed bed: prediction of breakthrough curves. *Process Biochemestry* 39 (2004) 599-613.
28. Bharathi, K.S.; Ramesh, S.P.T. Fixed-bed column studies on biosorption of crystal violet from aqueous solution by Citrullus Ianatus rind and Cyperus rotundus. *Applied Water Science* 3 (2013) 673-687.
29. Han, R.; Wang, Y.; Zhao, X.; Wang, Y.; Xie, F.; Cheng, J.; Tang, M. Adsorption of methylene blue by phoenix tree leaf powder in a fixed-bed column : experiments and prediction of breakthrough curves. *Desalination* 245 (2009) 284-297.

Please cite this Article as:
Mahdi K., Benrachedi K., Continuous flox adsorption of orange acid II by coffee grounds in fixed bed column, ***Algerian J. Env. Sc. Technology***, ***6*:3 (2020) 1466-1474**